

# Modelling and Simulation of the New Type of EMI Filter for Integrated Power Electronics Modules.

Piotr Rydlichowski<sup>#1</sup>, Wojciech Bandurski<sup>\*2</sup>

<sup>#</sup>Chair of Multimedia Telecommunication and Microelectronics, Poznań University of Technology  
ul. Polanka 3, 60-965 Poznań, Poland

<sup>1</sup>prydlich@et.put.poznan.pl

<sup>2</sup>wojciech.bandurski@et.put.poznan.pl

**Abstract**— Electromagnetic interference (EMI) at radio frequencies (RF) in compact integrated power electronic converter modules can be suppressed using lossy transmission line lowpass filters. Paper presents results of numerical simulations of proposed in [1] filter structure with modifications. Transfer function, current distribution and electromagnetic field distribution are considered. Structures are analyzed in full-wave electromagnetic simulator. Guidelines for further research is outlined.

## I. INTRODUCTION

In the following paper prototypes of a new planar lowpass filters are analyzed. Structures are shown in Fig. 1 (not in scale), Fig. 2, Fig. 3, Fig. 4 and Fig. 5. Main application of proposed structures is suppression of RF-EMI interference in power electronic devices. Such interferences are found mainly in integrated high power converters (power densities 13 W/cm<sup>3</sup> and above). Interferences are also caused by electromagnetic coupling between electronic devices during switching and by inductance and capacitance in electronic devices and in module package. In current structures used in aerospace industry filters are integrated (for convenience) with coaxial cables. With new technologies a need has occur to design new, small, planar lowpass filter for Integrated Power Electronic modules (IPEMs). Mentioned modules with kilowatt powers and high power densities can be a source of significant RF-EMI interferences. New filters for radio frequency (RF) modules must satisfy three main prerequisites: 1) because structure should be small the speed of electromagnetic wave must be reduced to fraction of its free-space velocity value, 2) structure should be electrically and mechanically able to handle power from 1 kW to 10 kW at 300 V to 500 V and 30A, 3) filter cut-off slope should be as steep as possible (e.g., > 40 dB/decade).

Prototype structure presented in [1] meets specified above requirements. Authors of this paper also present production technology of this kind of filter and experimental measurements of the transfer function are presented. This characteristics are compared with one obtained from proposed simple analytical modeling. This kind of filters have different forward and reverse characteristic, what is caused by geometry (as suggested by authors in [1]) and results in non uniform current density and EM field distribution in analyzed structure. As it was mentioned earlier transfer function is derived in forward and reverse direction. Obtained results -

Amplitude characteristics are different from experimental ones, especially in forward direction.

The goal of the following paper is to use a professional full-wave electromagnetic simulator to analyze this type of filters, especially current density for different frequencies. Scattering matrix  $S$  and admittance matrix  $Y$  for filter transfer function calculation in both forward and reverse direction are used.

## II. PARAMETERS OF ANALYZED STRUCTURES

Stepped filter structure [1] was chosen because of simple production and theoretical analysis. It is an approximation of exponential shape. Proposed structures are manufactured from several layers Cu - Al<sub>2</sub>O<sub>3</sub> - Ni - BaTiO<sub>3</sub> - Ni - Al<sub>2</sub>O<sub>3</sub> - Cu. Filter cross-section is presented on Fig. 6 (without - a and with - b common ground return). The Ni - BaTiO<sub>3</sub> - Ni layers are responsible for interferences reduction and it characteristics are main point of interest. Cu layers handle kW power levels. Unwanted higher order harmonics are diverted into Ni - BaTiO<sub>3</sub>- Ni layers were are finally suppressed. In [1] the following filter dimensions are considered: length - 100 mm, width of sections - 40 mm, 20 mm, 10 mm and 5 mm. Length of each section - 25 mm. Thickness: Ni - 17 μm,  $\sigma = 1,47 \cdot 10^7$  S/m and  $\mu_r = 100$ . BaTiO<sub>3</sub> layer - 150 μm,  $\tan \Delta = 0.0035 \sqrt{(f/10^6)}$  - approximation,  $\epsilon_r = 12000$ . Structure is simulated in 1 kHz - 100 MHz frequency range. Initial prototype filter structure was fabricated with uniform Ni layer shape. However non uniform Ni layer shape is characterized by desired higher attenuation. Because BaTiO<sub>3</sub> ceramic material is untypical its exact material parameters are not known, especially how do they change with temperature. These properties are also result of exact ceramic wafer fabrication from powder in sintering process. Proposed structures must handle significant power levels and also thermal properties should be considered.

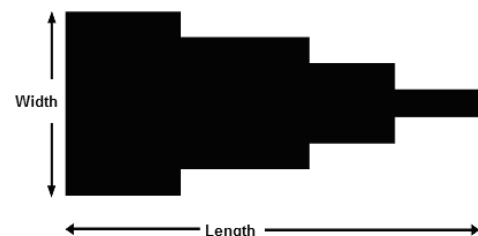


Fig. 1 Plan view of four-section Ni - BaTiO<sub>3</sub> - Ni attenuation layer [1]



Fig. 2 Plan view of linear Ni - BaTiO<sub>3</sub> - Ni attenuation layer



Fig. 3 Plan view of eight-section Ni - BaTiO<sub>3</sub> - Ni attenuation layer

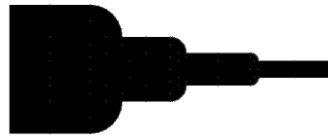


Fig. 4 Plan view of four-section, circularly shaped Ni - BaTiO<sub>3</sub> - Ni attenuation layer



Fig. 5 Plan view of exponentially shaped Ni - BaTiO<sub>3</sub> - Ni attenuation layer

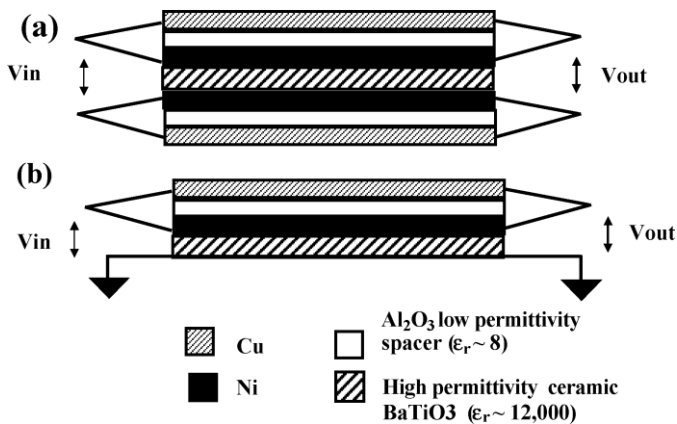


Fig. 6 Cross-section of analyzed filter structures [1]

Figures 2, 3, 4 and show proposed variations of structure on Fig. 1. In each structure terminals have same 40mm and 5mm width. Structure on Fig. 3 has following widths of each section: 40mm, 30mm, 20mm, 15mm, 10mm, 7.5mm, 6.5mm and 5mm. Structure on Fig. 4 has the same sections widths as structure on Fig. 1. Circular edges have 10mm, 5mm and 2.5mm radius respectively.

### III. ATTENUATION LAYER STRUCTURES SIMULATION

Professional full-wave electromagnetic simulator was used in simulations (IE3D package from Zeland [2]). It uses Method of Moments (MoM) to find discrete form of Maxwell equations. One of the most important parameter in presented simulations is meshing frequency. BaTiO<sub>3</sub> ceramic dielectric high  $\epsilon_r$  value determines meshing frequency for structure. This high dielectric constant value is responsible for slowing down propagating electromagnetic wave to fraction of its free-space velocity value and this also results in shorter wavelength. To obtain reasonably accurate results 15-20 mesh cells per wavelength are needed and this results in 12 GHz meshing frequency for analyzed structures. However simulations have shown that good accuracy is obtained already at 5 GHz. Higher meshing frequency and finite dielectric modeling gives better accuracy – more cells in structure but results in considerably longer simulation times. Research have shown that EM field simulators with accurate 3D dielectric modeling capabilities (most FDTD simulators) are better suited for considered structures than classical MoM simulator (because of high electrical permittivity difference between layers). Optimal simulation parameters must be determined by user and are a tradeoff between accuracy and simulation time. More information can be found in [3] and [4]. Presented structures on Fig. 1, Fig. 2, Fig. 3, Fig. 4 and Fig. 5 are simulated in common ground configuration. Proposed attenuator structure is untypical because of high dielectric permittivity which is not found in microstrip microwave filters. Physical and electrical parameters of dielectric material - BaTiO<sub>3</sub> are unsure. Recently new kind of material was proposed SrTiO<sub>3</sub> – it does not show dielectric constant relaxation phenomena. Stepped Ni structure is an approximation of exponential taper and is used because of simple production technology and simplified analytical approach as well. In order to explain Ni - BaTiO<sub>3</sub> - Ni attenuation characteristics we decided to find average current density and electromagnetic field distribution in and around the structure. Because of significant differences in electrical parameters between Ni and BaTiO<sub>3</sub> layers much care must be taken to properly analyze simulation results. The next stage was to calculate transfer function for each structure. Structure on Fig. 1 has already been analyzed, was fabricated and exact amplitude characteristic is known [1], [3] and [4]. Filter was simulated in the following configuration Fig. 7:

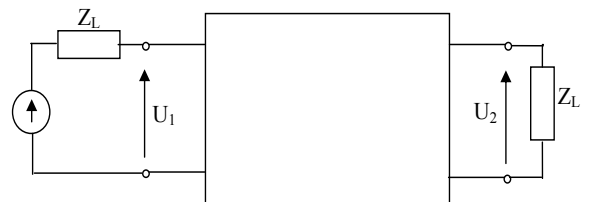


Fig. 7 Filter configuration used in simulations

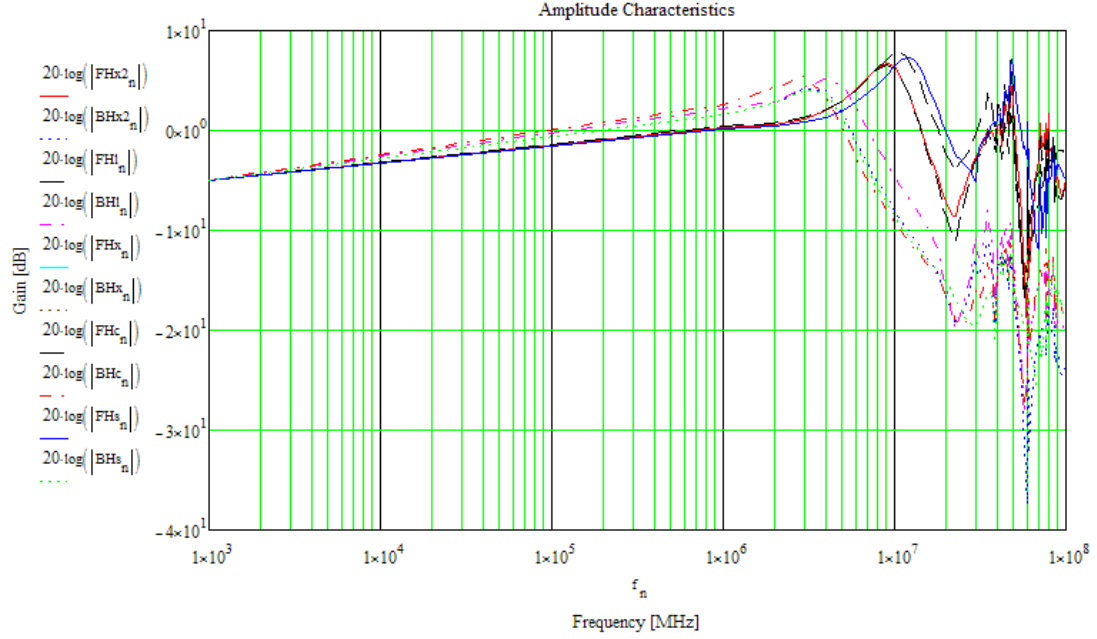


Fig. 9 Ni-BaTiO<sub>3</sub>-Ni attenuation structures amplitude characteristic

We are interested in amplitude characteristic for both forward -  $|H_F(\omega)|$  and reverse -  $|H_R(\omega)|$  direction. Transfer function  $H_F(\omega)$  and  $H_R(\omega)$  expressions:

$$H_F(\omega) = \frac{U_2(\omega)}{U_1(\omega)} = \frac{-Y_{21}}{Y_{22} + 1/Z_L}, H_R(\omega) = \frac{U_1(\omega)}{U_2(\omega)} = \frac{-Y_{12}}{Y_{11} + 1/Z_L}. \quad (1)$$

and amplitude characteristics (in dB) are given by:

$$A_F = 20 \log |H_F(\omega)|, A_R = 20 \log |H_R(\omega)|. \quad (2)$$

Similar procedure can be applied using  $S$  parameters. Both parameters  $Y$  and  $S$  are obtained in series of numerical simulations.

#### IV. SIMULATION RESULTS FOR Ni-BaTiO<sub>3</sub>-Ni ATTENUATION LAYER

The first stage was to simulate and analyze current density distribution for structures presented on Fig. 1 – Fig. 5. For lower frequencies 1 kHz – in pass-band we can observe current crowding effect. Another effect which can be observed is that current tends to flow near internal edges. For higher frequencies, 100 MHz we can observe skin depth effect and differences in current density for forward and backward directions. Fig. 8 presents experimental transfer function and best theoretical model obtained by authors in [1] for basic structure from Fig. 1. Detailed results with graphs for current distribution can be found in [4]. Fig. 9 presents amplitude characteristics calculated from  $Y$  matrix elements (from numerical simulations) for structures on Fig. 1 – Fig. 5.  $FH/BH$  mean forward and backward direction characteristic.

Suffixes  $s, l, x2, c$  and  $x$  describe structures from Fig. 1 – Fig. 5 respectively. No significant differences in amplitude characteristics between proposed geometries can be observed. It can be concluded that material properties, physical structure size and terminals size have the biggest influence on amplitude characteristics.

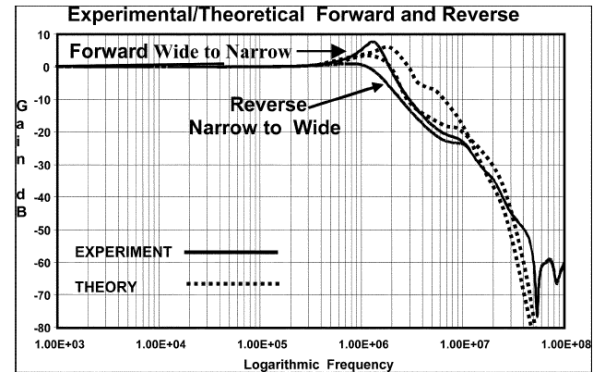


Fig. 8 Experimental and theoretical amplitude characteristics [1]

#### V. SIMULATION RESULTS FOR COMPLETE FILTER STRUCTURE.

The next stage was to simulate and analyze current density distribution and amplitude characteristic for complete filter structure presented on Fig. 6. Cu and Al<sub>2</sub>O<sub>3</sub> layers had 25 μm 0.65 mm in thickness respectively, loss factor for Al<sub>2</sub>O<sub>3</sub> 0.01 %. Amplitude characteristic, current distribution, electric and magnetic field distribution are presented on Fig. 9 - Fig. 15 respectively. It can be seen that simulations confirmed that signal is diverted and suppressed inside Ni layers for high frequencies.

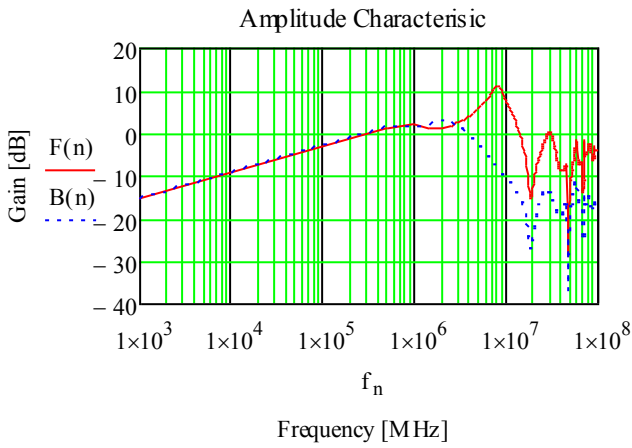


Fig. 9 Amplitude Characteristics for complete structure.

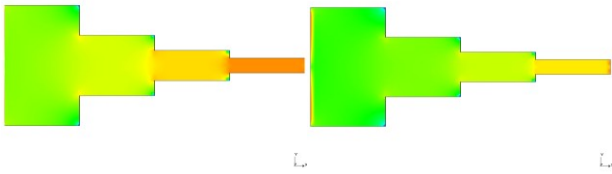


Fig. 10 Current distribution for Cu and Ni layer,  $f = 1$  kHz.

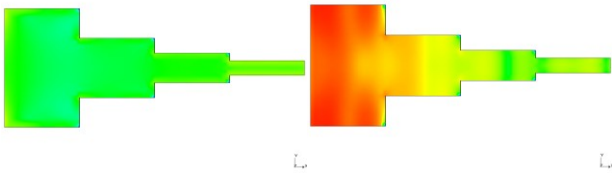


Fig. 11 Current distribution for Cu and Ni layer,  $f = 0.1$  GHz.

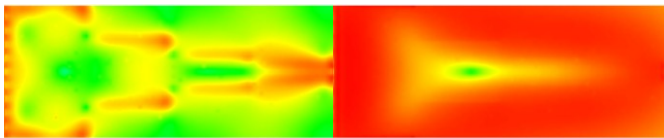


Fig. 12 Electric field for Cu and Ni layer,  $f = 1$  kHz.

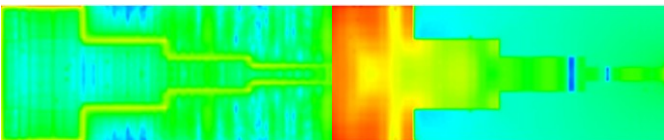


Fig. 13 Electric field for Cu and Ni layer,  $f = 0.1$  GHz.

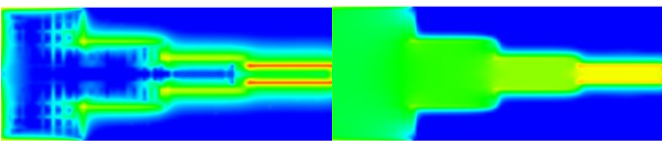


Fig. 14 Magnetic field for Cu and Ni layer,  $f = 1$  kHz.

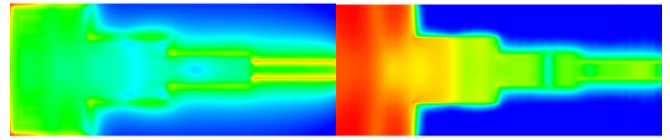


Fig. 15 Magnetic field for Cu and Ni layer,  $f = 0.1$  GHz.

## VI. ANALYTICAL MODELLING FOR COMPLETE FILTER STRUCTURE.

Initially authors in [3] used simple current crowding model to achieve better accuracy with experimental results. Authors of the following paper considered two analytical models. First one incorporates transverse resonance technique. This technique finds propagation constants for each layer. However obtained equations for considered structure cannot be solved analytically and further research in this area is required.

Second analytical approach is to find and synthesize equivalent circuit for each segment and for each step change in width. Such combined equivalent circuit can be modeled in PSpice software. Equivalent circuit parameters can be found using parameter extraction from numerical simulation results in IE3D. Untypical frequency range poses a problem in parameter extraction and wideband equivalent circuit is required. This is a point of further research.

## VII. CONCLUSIONS

Obtained simulation results confirmed expected effects inside considered structure. Derived amplitude characteristic for base structure is different from experimental one, especially in forward direction. Further research in modeling area is required. Better analytical model with accurate wideband parameter extraction also taking into account thermal aspects is required.

## REFERENCES

- [1] Colin Kydd Campbell, Jacobus Daniel van Wyk, Pieter Wolmarans, *Improved Transmission – Line Attenuators for Integrated Power Filters in the RF Band*, IEEE TRANSACTIONS ON COMPONENTS AND PACKAGING, VOL. 27, NO. 2, JUNE 2004 .
- [2] Zeland Corporation, *IE3D v. 10.0 Manual*, www.zeland.com (2002) .
- [3] Colin Kydd Campbell, Jacobus Daniel van Wyk, Rengang Chen, *Effect of Current Crowding on Frequency Response of a Stepped Planar RF Transmission-Line Lowpass Filter for Power Electronics*, IEEE TRANSACTIONS ON COMPONENTS AND PACKAGING, VOL. 29, NO. 4, NOVEMBER 2006.
- [4] Piotr Rydlichowski, Wojciech Bandurski, *Modeling of a new planar lowpass filter for Integrated Power Electronics Modules in IE3D simulator*, 18<sup>th</sup> INTERNATIONAL WROCLAW SYMPOSIUM AND EXHIBITION ON ELECTROMAGNETIC COMPATIBILITY, WROCLAW, 28 – 30 JUNE, 2006.